Smart Structures and Systems, *Vol. 12, No. 3-4 (2013) 441-463*
DOI:http://dx.doi.org/10.12989/sss.2013.12.3_4.441

Simplified planar model for damage estimation of interlocked caisson system

Thanh-Canh Huynh[1], So-Young Lee[1], Jeong-Tae Kim[*1], Woo-Sun Park[2] and Sang-Hun Han[2]

[1]Department of Ocean Eng., Pukyong National University, Busan, Korea
[2]Coastal Development and Ocean Energy Research Dept., Korea Institute of Ocean Science and Technology (KIOST), Ansan, Korea

(Received January 21, 2013, Revised June 29, 2013, Accepted July 14, 2012)

Abstract. In this paper, a simplified planar model is developed for damage estimation of interlocked caisson systems. Firstly, a conceptual dynamic model of the interlocked caisson system is designed on the basis of the characteristics of existing harbor caisson structures. A mass-spring-dashpot model allowing only the sway motion is formulated. To represent the condition of interlocking mechanisms, each caisson unit is connected to adjacent ones via springs and dashpots. Secondly, the accuracy of the planar model's vibration analysis is numerically evaluated on a 3-D FE model of the interlocked caisson system. Finally, the simplified planar model is employed for damage estimation in the interlocked caisson system. For localizing damaged caissons, a damage detection method based on modal strain energy is formulated for the caisson system.

Keywords: simplified model; interlocked caissons; modal strain energy; damage detection

1. Introduction

Caisson structures are usually designed for gravity-type breakwaters on foundation mounds. Over the last decades, severe failure events of caisson breakwaters have been reported from Japan, Italy, Spain, and Chile (Oumeraci 1994). Despite considerable lessons that have been learned from those failure events (Franco 1994, Oumeraci 1994, Tanimoto and Takahashi 1994), the structural failures have been observed in recent years (Maddrell 2005, Taro 2012). Meanwhile, structural health monitoring (SHM) has become the key to ensure the safety and serviceability of caisson breakwater systems. The adequate assessment of the structural safety and performance is prerequisite to estimate the failure probabilities for the design and maintenance of the breakwater system (Oumeraci *et al*. 2001).

Up to now, vibration-based damage monitoring for civil structures has been widely studied via examining the change in measured vibration response (Doebling *et al*. 1996, Sohn *et al*. 2003). The problems concerned with structural damage detection, localization and characterization can be solved by damage detection theories such as modal sensitivity method, modal flexibility method,

∗Corresponding author, Professor, E-mail: idis@pknu.ac.kr

http://www.techno-press.org/?journal=sss&subpage=8 ISSN: 1738-1584 (Print), 1738-1991 (Online)

genetic algorithm, and artificial neural network (Wu *et al*. 1992, Pandey and Biswas 1994, Kim and Stubbs 1995, Yun and Bahng 2000, Chou and Ghaboussi 2001, Koo *et al*. 2009, Park *et al*. 2009). Also, many sensor systems have been proposed for vibration-based SHM of civil structures. However, most of SHM systems have been applied to inland structures such as bridges and buildings (Wong 2004, Glisic *et al*. 2005, Jang *et al*. 2010, Ho *et al*. 2012). Many challenges still remain to develop efficient SHM systems for offshore structures such as breakwaters.

Over the past three decades, many researchers have investigated global structural failures of caisson-type breakwaters such as overturning, sliding or settlement by numerical analyses as well as experimental model tests (Yamamoto *et al*. 1981, Kobayashi *et al*. 1987, Sekiguchi and Ohmaki 1992, Sekiguchi and Kobayashi 1994). A few researchers have analyzed vibration responses of coastal structures considering soil-structure or fluid-soil-structure interactions (Yang *et al*. 2001, Kim *et al*. 2005). Recently, a few researchers have attempted to monitor the health status of caisson structures using changes in modal parameters (Park *et al*. 2011, Lee *et al*. 2011, 2012, Yoon *et al*. 2012). Those studies have mostly concentrated on mono-caisson systems which have potential damage in structure-foundation interface. For damage assessment in a real caisson breakwater, the following main issues should be considered: (1) the submerged condition of the coastal structure limits the accessibility for vibration measurement; and (2) the harbor caisson system consists of multiple caisson segments which are normally interconnected with each other by shear-keys to resist against the incident wave force acting perpendicular to the front wall.

In this study, a simplified planar model is presented to estimate damage in the interlocked caisson system. Firstly, a conceptual dynamic model of the interlocked caisson system is designed on the basis of the characteristics of existing harbor caisson structures. A mass-spring-dashpot model allowing only the sway motion is formulated. To represent the condition of interlocking mechanisms, each caisson unit is connected to adjacent ones via springs and dashpots. Secondly, the accuracy of the planar model concept for vibration analysis is numerically evaluated on a 3-D FE model of interlocked caissons. Finally, the simplified model is employed to estimate damage in the caisson system. A damage detection method based on modal strain energy is formulated to localize damage in the caisson system.

2. Planar model of interlocked caissons

2.1 Equations of motion

As shown in Fig. 1, the caisson system is subjected to an impulsive breaking wave force that results in forced vibration responses. Since the wave action is usually perpendicular to the caisson array axis (i.e., x-direction), the vibration in the impact direction (i.e., y-direction) is relatively larger than other directions (Lee *et al*. 2011, 2012, Yoon *et al*. 2012). Therefore, only the sway motion of caissons (i.e., y-direction) is taken into account in this study. Based on a few existing simplified models (Smirnov and Moroz 1983, Marinski and Oumeraci 1992, Goda 1994, Oumeraci and Kortenhaus 1994, Vink 1997), a planar model of three interlocked caissons is proposed as shown in Fig. 2. In the simplified model, caissons are treated as rigid bodies on elastic half-space foundations which can be described via the horizontal springs and dashpots. To represent the condition of interlocking mechanism, springs and dashpots are also simulated between adjacent caissons.

By equating to the equilibrium conditions of the free-body diagrams of caissons (see Fig. 2),

the sway motion can be formulated in matrix form as

$$\begin{bmatrix} m_1 & 0 & 0 \\ 0 & m_2 & 0 \\ 0 & 0 & m_3 \end{bmatrix} \begin{Bmatrix} \ddot{u}_1 \\ \ddot{u}_2 \\ \ddot{u}_3 \end{Bmatrix} + \begin{bmatrix} c_{F1}+c_{S1}+c_{S2} & -c_{S2} & 0 \\ -c_{S2} & c_{F2}+c_{S2}+c_{S3} & -c_{S3} \\ 0 & -c_{S3} & c_{F3}+c_{S3}+c_{S4} \end{bmatrix} \begin{Bmatrix} \dot{u}_1 \\ \dot{u}_2 \\ \dot{u}_3 \end{Bmatrix} + \begin{bmatrix} k_{F1}+k_{S1}+k_{S2} & -k_{S2} & 0 \\ -k_{S2} & k_{F2}+k_{S2}+k_{S3} & -k_{S3} \\ 0 & -k_{S3} & k_{F3}+k_{S3}+k_{S4} \end{bmatrix} \begin{Bmatrix} u_1 \\ u_2 \\ u_3 \end{Bmatrix} = \begin{Bmatrix} P_1(t) \\ P_2(t) \\ P_3(t) \end{Bmatrix} \tag{1}$$

where m_j is the total horizontal mass of the j^{th} caisson; k_{Fj} and c_{Fj} separately represent the horizontal spring and dashpot of the j^{th} caisson's foundation (j=1-3); k_{Fj} and c_{Fj}, respectively, represent the horizontal spring and dashpot of the k^{th} shear-key connection (k=1-4); $\ddot{u}_j, \dot{u}_j$ and u_j are, respectively, the horizontal acceleration, velocity and displacement of the j^{th} caisson; and $P_j(t)$ is the external force placed at the center of gravity of the j^{th} caisson.

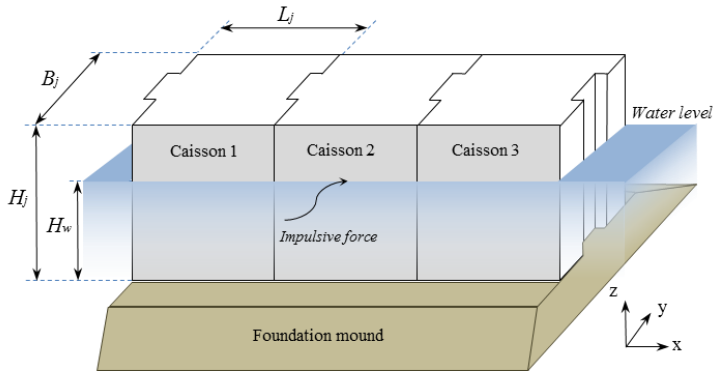

Fig. 1 A caisson system of three units

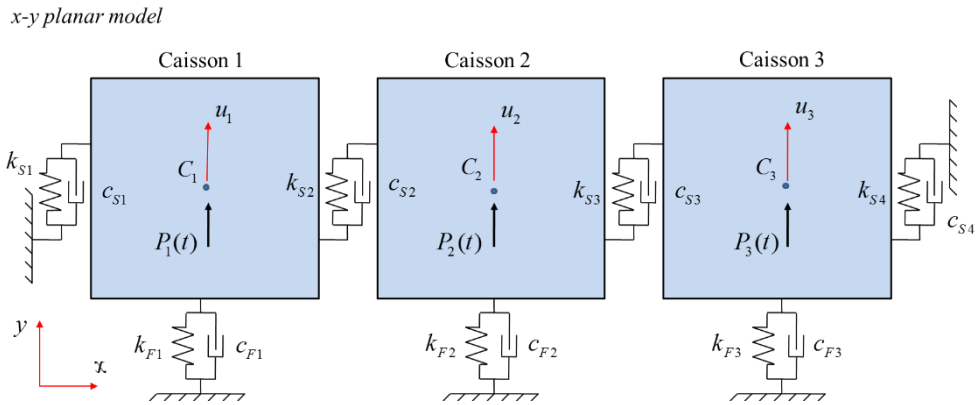

Fig. 2 Simplified dynamic model of three interlocked caissons

2.2 Determination of structural parameters

2.2.1 Mass parameter

When the caisson is oscillated by an impact load, the surrounding media (i.e., soil and water) are forced to move with the structure. Therefore, the total horizontal mass of the j^{th} caisson (m_j) includes not only the mass of the caisson ($m^{cai}{}_j$) but also the horizontal hydrodynamic ($m^{hyd}{}_j$) and the horizontal geodynamic masses ($m^{geo}{}_j$) as follows

$$m_j = m_j^{cai} + m_j^{hyd} + m_j^{geo} \tag{2}$$

For calculating the horizontal hydrodynamic mass, the equation presented by Oumeraci and Kortenhaus (1994) is used

$$m_j^{hyd} = 0.543 L_j \rho_w H_w{}^2 \tag{3}$$

in which the quantities L_j and H_w represent the j^{th} caisson's length and the water level, as shown in Fig. 1; and the quantity ρ_w is the mass density of sea water.

According to Richart et al. (1970), the horizontal geodynamic mass can be computed as

$$m_j^{geo} = 0.76 \rho_s \left(\frac{B_j L_j}{\pi} \right)^{3/2} /(2 - \nu) \tag{4}$$

where ρ_s and ν are respectively the mass density and Poisson's ratio of the foundation soil; and B_j is the j^{th} caisson's width, as sketched in Fig. 1.

2.2.2 Stiffness parameter

It is commonly accepted in geotechnical engineering that the horizontal spring constant (k_{Fj}) of the elastic foundation is the function of the horizontal modulus of subgrade reaction *(b)* as, the j^{th} caisson width (B_j) and length (L_j), follows

$$k_{Fj} = b L_j B_j \tag{5}$$

The modulus of subgrade reaction of various soil types, which has the unit of pressure per length, can be found in literature by Bowles (1996). The same formulas have also been adopted by Goda (1994) and Vink (1997).

Unlike the foundation mound, the theoretical basis for determination of the shear-keys' stiffness is weaker since it depends on the linking capacity between contacted units in the real caisson breakwater (Lamberti and Martinelli 1998, Oumeraci *et al*. 2001). Normally, caisson segments are designed with the uniform linking capacity, where $k_{S2} = k_{S3}$. Since the rest of caisson array is not represented in the planar model, the stiffness of the last shear-keys (i.e., k_{S1} and k_{S4}) is smaller than that of the middle shear-keys (i.e., k_{S2} and k_{S3}). This condition can be expressed as:

$$k_{S1} = k_{S4} = a k_{S2} = a k_{S3} \tag{6}$$

where a is an empirical value ranging from 0 to 1 (Lamberti and Martinelli 1998). In computation, the stiffness parameters are obtained by adjusting the vibration responses of the simplified model to fit those of the 3-D FE model.

2.2.3 Damping parameter

In this study, the Rayleigh damping, which is often used in the dynamic mathematical model, is used to simulate the energy dissipation in the caisson system. The Rayleigh damping is assumed to be proportional to the mass and stiffness matrices (Wilson 2004)

$$[C] = \alpha[M] + \beta[K] \tag{7}$$

in which α is the mass-proportional damping coefficient; and β is the stiffness-proportional damping coefficient. Due to the orthogonality conditions of the mass and stiffness matrices, this equation can be rewritten as

$$\xi_n = \frac{1}{2\omega_n}\alpha + \frac{\omega_n}{2}\beta \tag{8}$$

where ξ_n is the critical-damping ratio for mode n; and ω_n is the n^{th} natural frequency.

If the damping ratios (e.g., ξ_i and ξ_j) corresponding to two specific frequencies (e.g., ω_i and ω_j) are known, the two Rayleigh damping factors (i.e., α and β) can be evaluated from the following equation

$$\begin{bmatrix} \xi_i \\ \xi_j \end{bmatrix} = \frac{1}{2}\begin{bmatrix} \frac{1}{\omega_i} & \omega_i \\ \frac{1}{\omega_j} & \omega_j \end{bmatrix}\begin{bmatrix} \alpha \\ \beta \end{bmatrix} \tag{9}$$

When damping ratios for both frequencies are set to an equal value, $\xi_i = \xi_j = \xi$, the Rayleigh damping factors are calculated as (Wilson 2004)

$$\beta = \frac{2\zeta}{\omega_i + \omega_j} \qquad \text{and} \qquad \alpha = \omega_i\omega_j\beta \tag{10}$$

3. Validation of planar model for vibration analysis

3.1 Target caisson structure

A lab-scaled caisson system consisting of three concrete caisson modules (i.e., Caisson 1, Caisson 2 and Caisson 3) was chosen as the target caisson structure. The geometry of the target caisson-type breakwater is sketched in Fig. 3. As shown in the figure, caissons are designed with shear-key connections to prevent them from shear motions. The caissons are filled with sand and covered by concrete caps with the thickness of 0.06 m. The width, height and length of a caisson unit are 0.34 m, 0.4 m and 0.34 m, respectively. The foundation consists of a 0.08 m thick mound of medium-dense sand and a 0.02m thick layer of medium gravel. The whole caisson system is placed on the sea bed of dense sand. The water depth measured from the sea bed at both sides of the caisson system is 0.44 m.

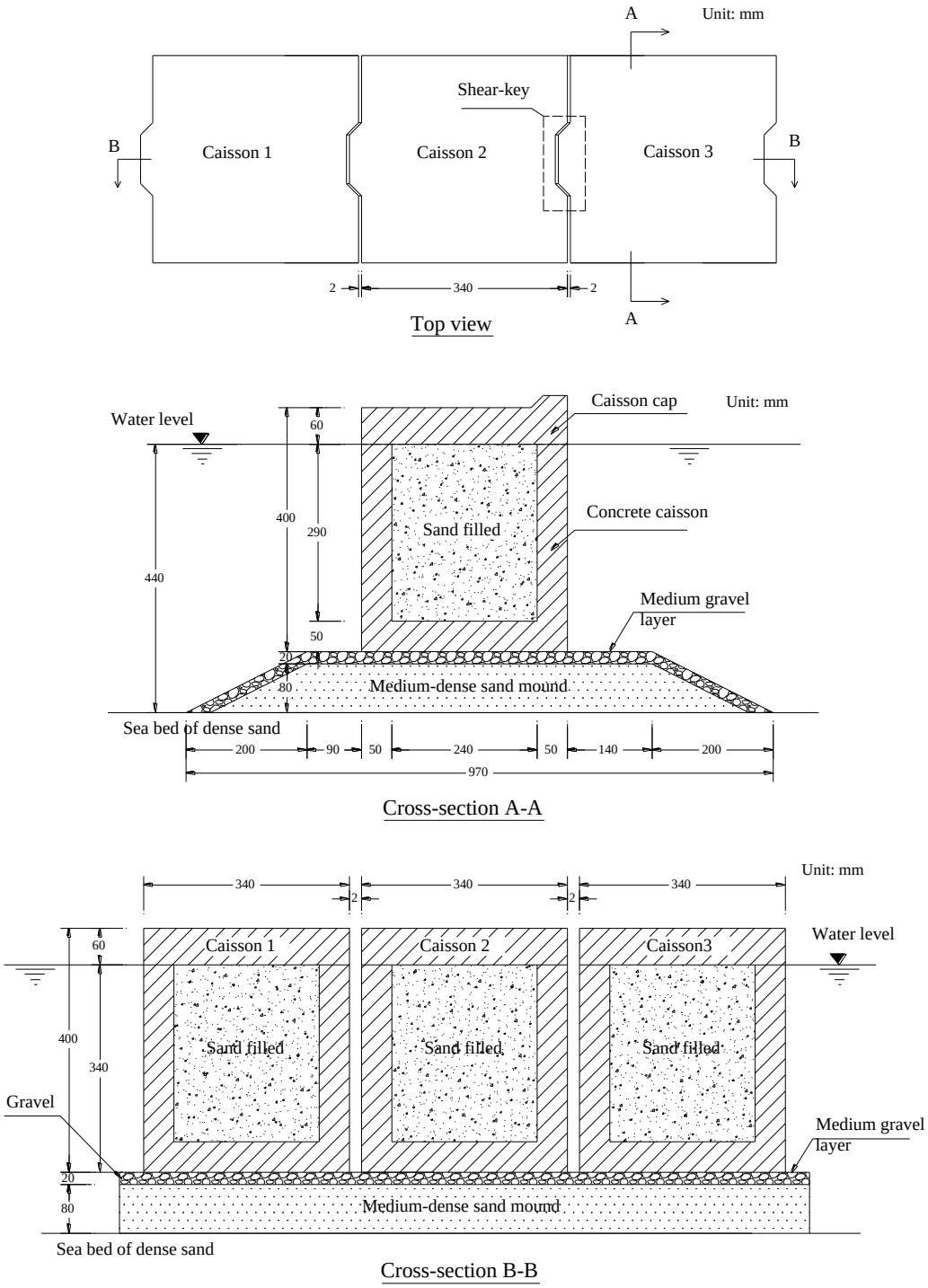

Fig. 3 Geometry of target caisson structure

A 28-day compressive strength of 28 MPa, an elastic modulus of 24 GPa and a Poisson's ratio of 0.2 are designed for concrete caissons. For foundation soils (i.e., medium-dense sand and medium gravel), soil parameters are selected according to the geotechnical engineering handbook by Look (2007). The material properties of the target caisson structure are provided in Table 1.

Table 1 Material properties of target caisson structure

	Concrete	Medium-dense sand	Medium gravel
Mass density (kg/m^3)	2400	2000	2100
Elastic modulus (MPa)	24000	30	50
Poisson's ratio	0.2	0.325	0.3

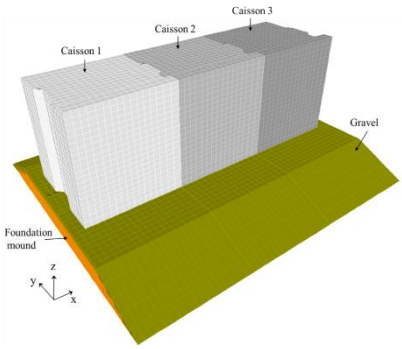

(a) 3-D FE model

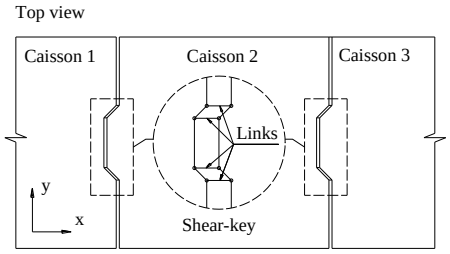

(b) Interlocking conditions

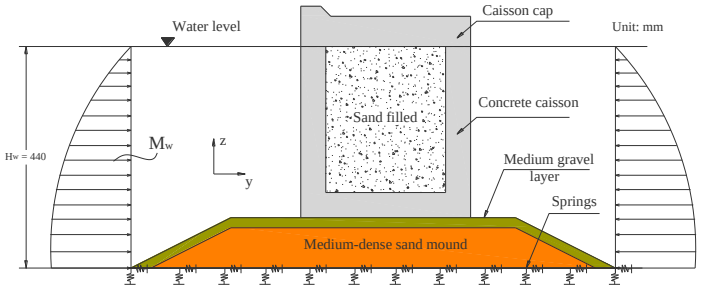

(c) Boundary conditions

Fig. 4 3-D FE model of target caisson structure

3.2 3-D FE analysis of target caisson structure

3.2.1 3-D FE Model

A 3-D FE model of the target caisson structure is simulated using SAP2000 software as shown in Fig. 4(a). In the 3-D FE model, the elastic characteristic of the sea bed (dense sand) is described by an area spring system (see Fig. 4(c)). According to the previous experimental studies on foundation analysis by Bowles (1996), the spring constant for dense sand is recommended to be 64 to 128 MN/m/m^2. Therefore, 96 MN/m/m^2 is selected for the spring constant of the sea bed. The interlocking condition is simulated by y-directional 1-D links at the shear-keys, as shown in Fig. 4(b). In this study, the stiffness of links is assumed to be 25 MN/m/m^2. Due to additional hydrodynamic damping effects, the damping ratios of caisson breakwaters are relatively higher than those of general concrete structures (e.g., 3%). In the previous experimental studies by Gao *et al*. (1988), the damping ratios of real caisson structures were found to be 3.2-7.5%. Hence, 5% of the damping ratio is assumed for all modes in the 3-D FE model.

To simulate the submerged condition of the target caisson structure, the effective mass of sea water (M_w) is added to the 3-D numerical model, as shown in Fig. 4(c). The added mass of sea water is calculated by Westergaard's hydrodynamic water pressure equation (Westergaard 1933) as follows

$$M_w = \int_{h_1}^{h_2} \frac{7}{8} \rho_w \sqrt{H_w h} \, .dh \tag{11}$$

where M_w is the hydrodynamic mass; ρ_w is the water density; H_w and h are the depth from water level to the foundation and that to the action point of hydrodynamic pressure, respectively. It should be noted that Eq. (3) is a simplified form of Eq. (11) when $h_1 = 0$ and $h_2 = H_w$.

In order to obtain vibration responses of the caisson system, forced vibration analysis is designed considering limited accessibilities. An impact force, which has corresponding direction of incident wave (i.e., y-direction), is applied perpendicularly to the front wall of Caisson 2 as denoted in Fig. 5. The impact force is assumed to be a half sine function with 10N-power and 0.01s-duration. The y-directional acceleration responses are measured at nine points (i.e., 1-9) on the top of the caisson caps as shown in Fig. 5. The sampling frequency is set as 1 kHz.

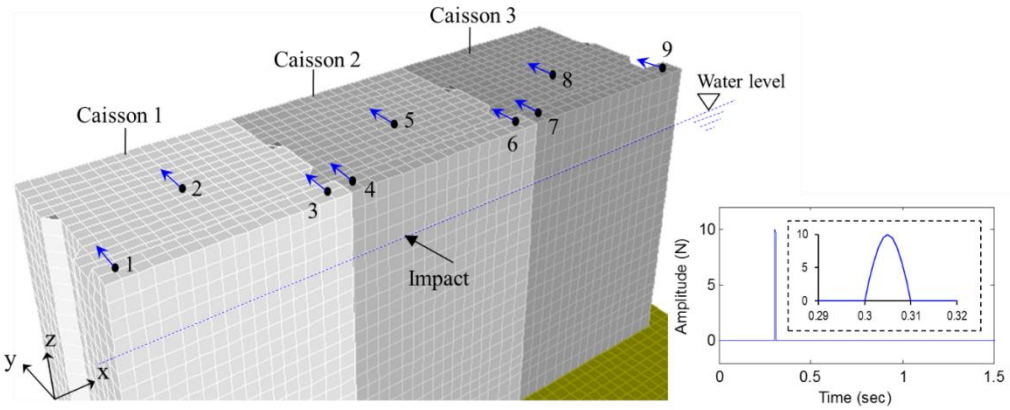

Fig. 5 Impact excitation and acceleration acquisition points

Fig. 6 shows acceleration signals in y-direction of points 2, 5 and 8. It is observed that the vibration of Caisson 2 is propagated into Caisson 1 and Caisson 3. However, the vibration amplitude of the unexcited caisson are only about a half of that of the excited one. This implies that a certain amount of energy is apparently subtracted from the excited caisson by wave propagation along the caisson system. This observation is similar to previous experimental studies reported by Lamberti and Martinelli (1998).

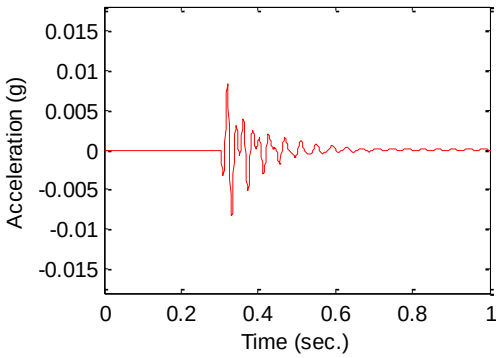

(a) Point 2 (Caisson 1)

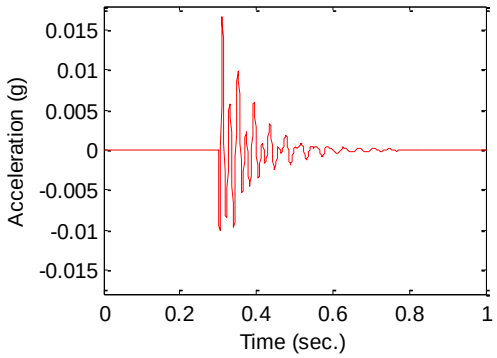

(b) Point 5 (Caisson 2

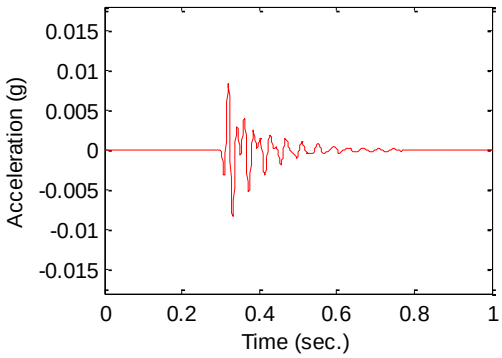

(c) Point 8 (Caisson 3)

Fig. 6 Y-directional acceleration signals of 3-D FE model

3.2.2 Vibration modal analysis

The frequency domain decomposition (FDD) method (Otte *et al*. 1990, Yi and Yun 2004) is used to extract modal parameters such as natural frequency and mode shape. The singular values of the power spectral density (PSD) function matrix $S(\omega)$ are used to estimate the natural frequencies instead of the PSD functions themselves as follows

$$S(\omega) = U(\omega)^T \Sigma(\omega) V(\omega) \tag{12}$$

where Σ is the diagonal matrix consisting of the singular values (σ_i's) and U and V are unitary matrices. Since $S(\omega)$ is symmetric, U becomes equal to V. In the FDD method, the natural

frequencies can be determined from the peak frequencies of the singular value, and the mode shape from anyone of the column vectors of $U(\omega)$ at the corresponding peak frequencies. Generally, the first singular value $\sigma_1(\omega)$ among σ_i's (i=1,…, N) is used to estimate the modal parameters except in some special cases such as with two or more identical excitations.

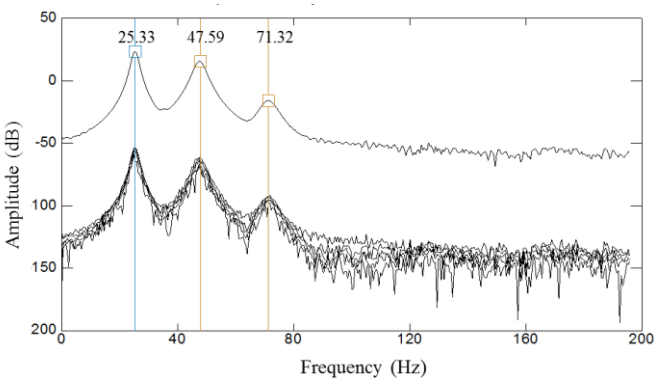

Fig. 7 Singular values of FDD procedure for 3-D FE model

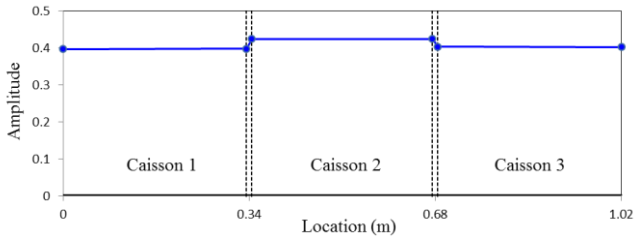

(a) Mode 1

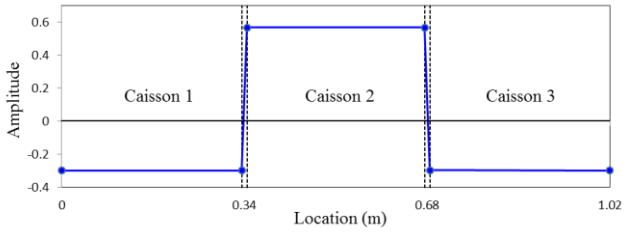

(b) Mode 2

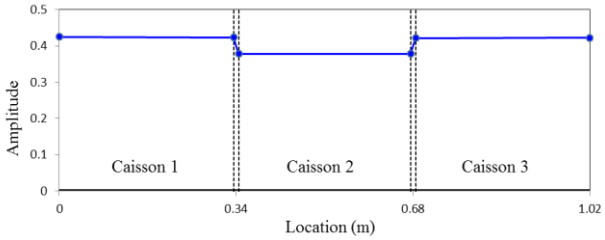

(c) Mode 3

Fig. 8 Y-directional mode shapes of 3-D FE model

The y-directional acceleration responses measured at points 1, 3, 4, 6, 7 and 9 on the top of the caissons (see Fig. 5) are used to extract natural frequencies and mode shapes of the 3-D FE model.

The singular values of the FDD procedure are shown in Fig. 7. In the frequency range of 0-200 Hz, three peaks that are selected for the target modes are 25.33 Hz, 47.59 Hz and 71.32 Hz, as listed in Table 2. The corresponding mode shapes are shown in Fig. 8. It is noted in the figure that the three caissons mostly move together in the same phase for mode 1 and mode 3 while the opposite phase is observed for the mode 2.

Table 2 Natural frequencies of 3-D FE model

Natural frequency (Hz)		
Mode 1	Mode 2	Mode 3
25.33	47.59	71.32

3.3 Planar model of 3-D FE simulation

The 3-D FE model of the target caisson structure is simplified using the proposed theoretical model. The impulsive load (see Fig. 5) is applied only on Caisson 2 in the simplified model. The total horizontal masses are computed as $m_1 = m_2 = m_3 = 149.52$ kg by using Eqs. (2) - (4). The total horizontal mass includes the mass of concrete, the mass of sand filled, the added masses of sea water, and the added mass of foundation soil. The stiffness parameters are determined by matching vibration responses of the simplified model and the 3-D FE model using try-and-error method.

The modulus of subgrade reaction of the foundation mound is selected as $25\text{x}10^6$ N/m^3 which is equivalent with that of medium dense sand (Bowles 1996). By using Eq. (5), the spring constants of the foundation mound are calculated as $k_{F1} = k_{F2} = k_{F3} = 2.89\text{x}10^6$ N/m. By assuming $k_{S1} = k_{S4} = 0.5k_{S2} = 0.5k_{S3}$ (Martinelli and Lamberti 2011), the stiffness of the middle and last shear-keys are obtained as $k_{S2} = k_{S3} = 3.179\text{x}10^6$ N/m and $k_{S1} = k_{S4} = 1.59\text{x}10^6$ N/m, respectively.

For calculating the damping parameter, the first two natural frequencies ($f_1 = 25.33$ Hz and $f_2 = 47.59$ Hz) and the critical damping ratio (5%) of the 3-D FE model are utilized to calculate the two Rayleigh damping coefficients (see Eq. (10)). The calculated mass-proportional damping coefficients (α) and stiffness-proportional damping coefficient (β) are, respectively, 10.387 and 0.000218.

To solve the equations of motion, the Runge–Kutta scheme supported in Matlab R2012b is utilized (Press *et al*. 1988). In the calculation process of vibration responses, the time interval is selected as 0.001 second.

3.4 Validation of simplified Model for vibration analysis

3.4.1 Vibration response in time domain

It is noted that the acceleration acquisition coordinate used in the simplified model is differed from that in the 3-D FE model, as described in Fig. 9. In the 3-D FE model, acceleration signals on the top of caissons are measured, whereas acceleration signals of the simplified model are computed at the mass centroids of the caissons. The difference in acceleration acquisition coordinates causes the difference in amplitudes of acceleration signals obtained from the simplified model and the 3-D FE model, as shown in Fig. 10. The vibration amplitudes of the

simplified model are only about half of those of the 3-D FE model. To validate the accuracy of the simplified model in vibration analysis, the acceleration signals of the simplified model should be compared with those measured at the caissons' centroids of the 3-D FE model. However, it is almost impossible to measure directly these signals from real caisson breakwaters.

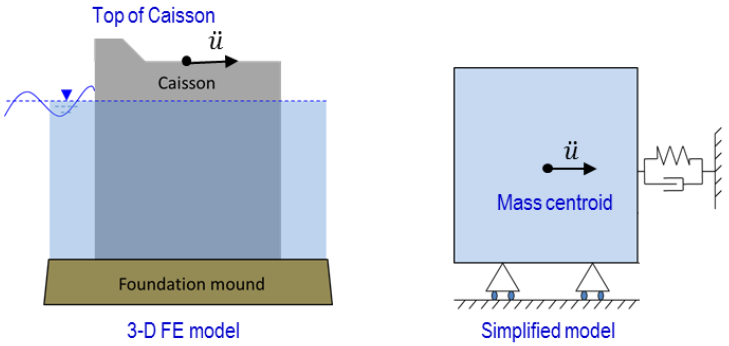

Fig. 9 Difference in acceleration acquisition coordinates between 3-D FE model and simplified model

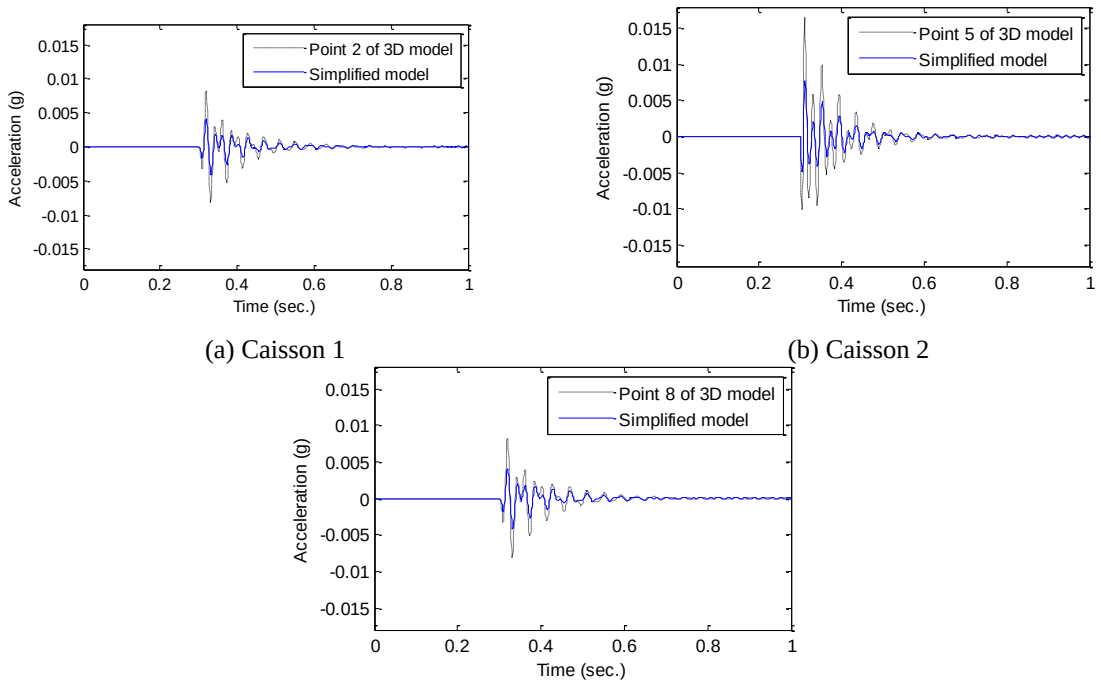

(a) Caisson 1 (b) Caisson 2

(c) Caisson 3

Fig. 10 Y-directional acceleration signals of 3-D FE model and simplified model with different acceleration acquisition coordinates

In order to match the acceleration acquisition coordinates between the simplified model and the 3-D FE model, the following procedure is performed by estimating the acceleration signals of the mass centroids of the caissons from the ones measured on the caisson caps in the 3-D FE model. Firstly, y-directional acceleration signals of additional locations on the front walls (i.e., points 10, 11 and 12) are measured as shown in Fig. 11(a). By comparing the acceleration signals of the upper points (i.e., 3, 6 and 9) and the lower points (i.e., 10, 11 and 12), the inclinations of the caissons can be obtained. Secondly, the mass centroid of each caisson is computed considering the added mass of sea water by Eq. (3) and added mass of soil by Eq. (4), as indicated in Fig. 11b. Thirdly, for each caisson unit, the acceleration signal of the mass centroid (i.e., C_1, C_2 or C_3) is linearly-estimated based on its inclination (i.e., α_1, α_2 or α_3) and the measured signal at the top center location (i.e., point 2, point 5 or point 8).

Fig. 12 shows the comparison between the estimated y-directional acceleration signals and the true ones of the caissons' centroids. It is noted that the true signals are measured directly at the caissons' centroids in the 3-D FE model. As observed in the figure, the estimated signals show good agreement with the true ones. Next, the estimated y-directional acceleration signals at the caissons' centroids in the 3-D FE model are used to compare with those of the simplified model, as sketched in Fig. 13. It can be seen in the figure that the signals of both models are well-matched.

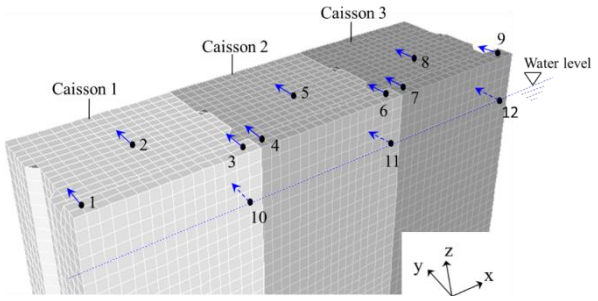

(a) Additional acceleration acquisition points 10, 11 and 12

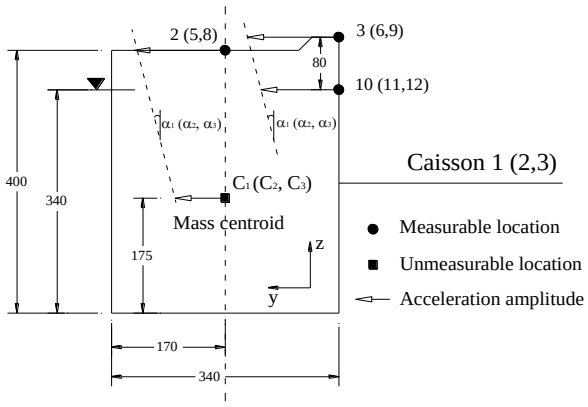

(b) Linear relationships of acceleration signals

Fig. 11 Estimation of y-directional acceleration signals of caissons' centroids

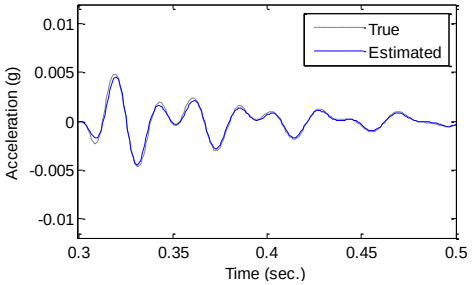

(a) Centroid of Caisson 1

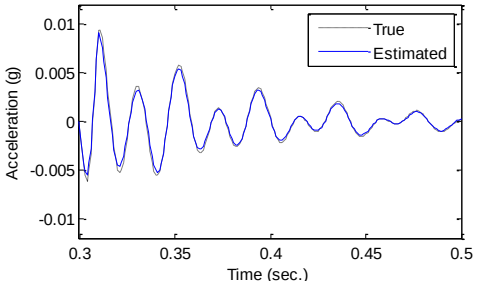

(b) Centroid of Caisson 2

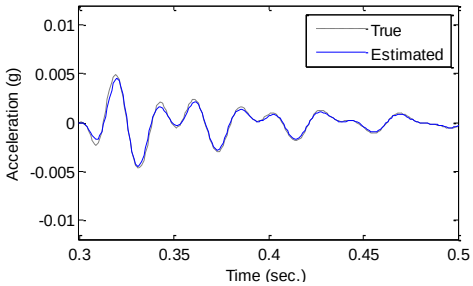

(c) Centroid of Caisson 3

Fig. 12 Y-directional acceleration signals at caissons' centroids in 3-D FE model

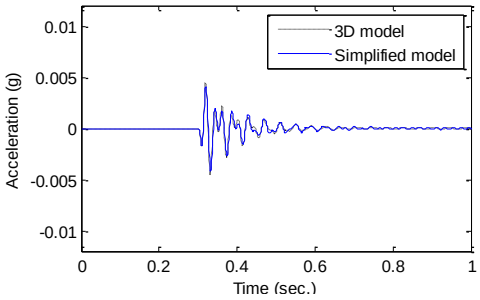

(a) Centroid of Caisson 1

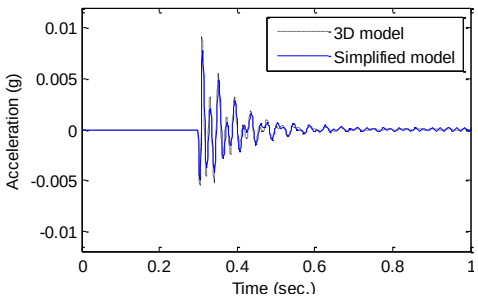

(b) Centroid of Caisson 2

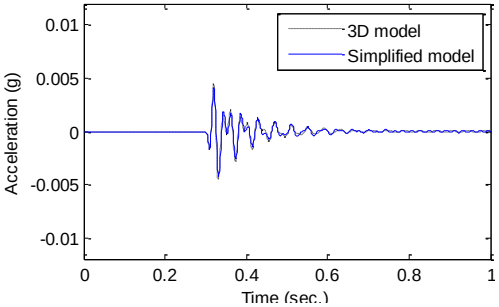

(c) Centroid of Caisson 3

Fig. 13 Y-directional acceleration signals of 3-D FE model and simplified model with equivalent acceleration acquisition coordinates

3.4.2 Vibration response in frequency domain

The PSDs of y-directional acceleration signals of the caissons' centroids are computed using Fast Fourier Transform (FFT) for the both models (i.e., simplified model and 3-D FE model), as shown in Fig. 14. It can be seen that the magnitudes and frequencies of the first two peaks obtained from the two models are well-matched. The FDD method (Otte *et al*. 1990, Yi and Yun 2004) is performed to extract modal parameters from the acceleration signals. The extracted mode shapes and corresponding natural frequencies are sketched in Fig. 15 and given in Table 3, respectively. It can be seen that the modal parameters of the simplified model are similar to those of the 3-D FE model.

In order to improve the understanding of mode shapes of target caisson structure, modal analysis of the 3-D FE model is carried out in SAP2000 software. The first and second mode shapes of the target caisson breakwater are shown in Fig. 16. It is observed that three caissons mostly move together in the same phase for the first mode, but in the opposite phase for the second mode. These results are well comparable with those sketched in Fig. 15.

From these above observations, it is concluded that the simplified model of the interlocked caissons successfully represents the horizontal vibrations of the 3-D FE model. Hence, the proposed model can be used for dynamic analysis of interlocked caisson systems.

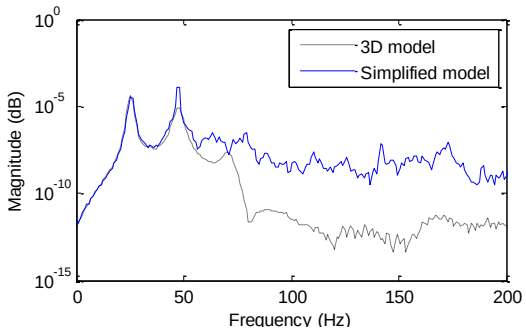

(a) Centroid of Caisson 1

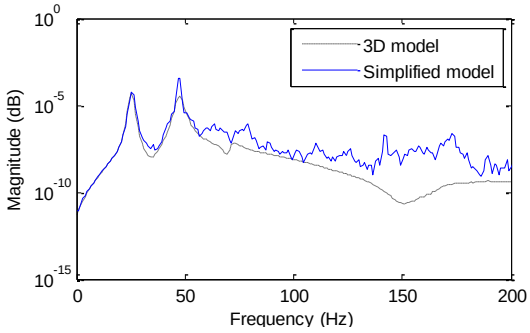

(b) Centroid of Caisson 2

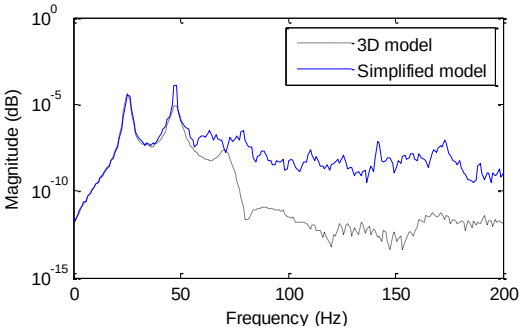

(c) Centroid of Caisson 3

Fig. 14 The PSDs of y-directional acceleration signals of 3-D FE model and simplified model

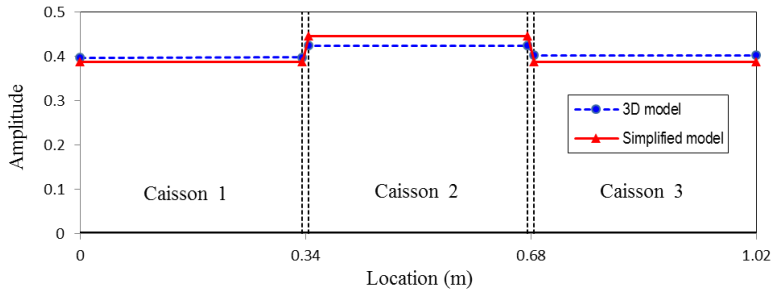

(a) Mode 1

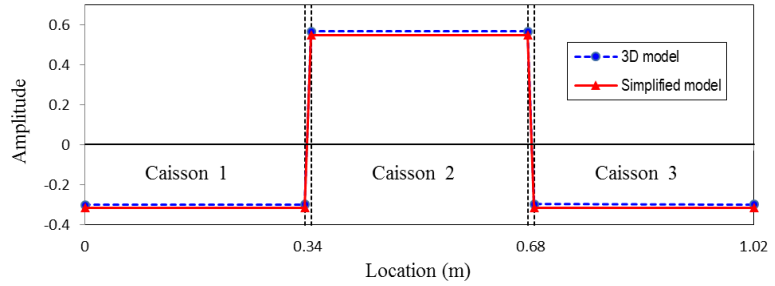

(b) Mode 2

Fig. 15 Y-directional mode shapes of 3-D FE model and simplified model

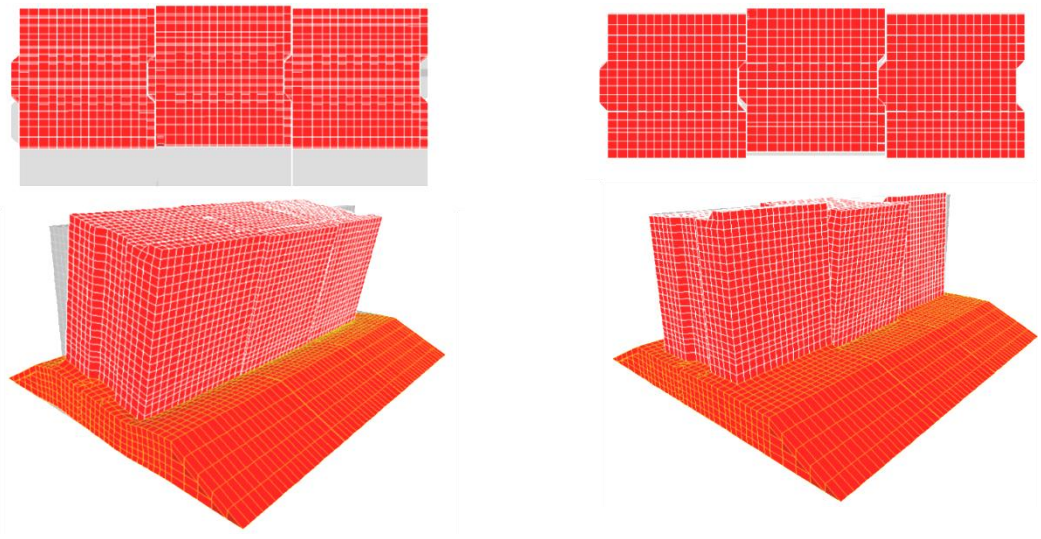

(a) Mode 1 (b) Mode 2

Fig. 16 Mode shapes of 3-D FE model by modal analysis

Table 3 Natural frequencies of 3-D FE model and simplified model

Mode	Natural frequency (Hz)		
	FE model	Simplified model	Difference
Mode 1	25.33	25.88	2.13%
Mode 2	47.59	47.36	-0.49%

4. Feasibility of planar model for damage estimation

4.1 Modal strain energy-based damage detection

The simplified model of the interlocked caissons is utilized to design a damage detection model on the basis of the MSE-based damage detection method (Kim and Stubbs 2002). For a linear, undamaged caisson system, as shown in Fig. 2, the i^{th} modal strain energy, U_i, is written by

$$U_i = \frac{1}{2}\sum_{j=1}^{nc}\phi_{ij}^2 k_{F_j} + \frac{1}{2}\sum_{j=1}^{n}(\phi_{ij} - \phi_{ij-1})^2 k_{S_j} \tag{13}$$

where nc is the number of caisson units; n is the number of shear-key connections; ϕ_{ij} is the i^{th} modal displacement at the j^{th} caisson; k_{Fj} represents the stiffness of the j^{th} caisson's foundation; and k_{Sj} is the stiffness of the j^{th} shear-key connection.

The contribution of the j^{th} caisson's foundation to the i^{th} modal strain energy, U_{ij}, is defined as

$$U_{ij} = \frac{1}{2}\phi_{ij}^2 k_{F_j} \tag{14}$$

Then, the fraction of the undamaged modal strain energy (i.e., the undamaged modal sensitivity) of the i^{th} mode and the j^{th} caisson is given by

$$F_{ij} = \frac{U_{ij}}{U_i} \tag{15}$$

For the caisson system with only foundation damage, the damaged modal sensitivity of the i^{th} mode and the j^{th} caisson can be expressed as

$$F_{ij}^* = \frac{U_{ij}^*}{U_i^*} \tag{16}$$

in which the quantities U_{ij}^* and U_i^* are calculated by

$$U_{ij}^* = \frac{1}{2}\phi_{ij}^{*2} k_{F_j}^* \tag{17}$$

$$U_i^* = \frac{1}{2}\sum_{j=1}^{nc}\phi_{ij}^{*2} k_{F_j}^* + \frac{1}{2}\sum_{j=1}^{n}(\phi_{ij}^* - \phi_{ij-1}^*)^2 k_{S_j} \tag{18}$$

For damage localization in the caisson system, a damage index η_j for the j^{th} caisson is defined via the ratio between the relative change in the modal sensitivity for the i^{th} mode with respect to the j^{th} caisson and the relative change in the stiffness of the j^{th} caisson's foundation as follows

$$\eta_j = \frac{F_{ij}^* / F_{ij}}{k_{F_j}^* / k_{F_j}} \tag{19}$$

in which η_j >1 indicates damage at the j^{th} caisson.

On substituting Eqs. (14)-(17) into Eq. (19), and by rearranging, the damage localization index η_j of the j^{th} caisson is simplified as the following

$$\eta_j = \frac{\phi_{ij}^{*2} U_i}{\phi_{ij}^2 U_i^*} \tag{20}$$

in which the i^{th} modal strain energies of pre- and post-damage cases can be expressed as

$$U_i = \frac{1}{2}\lambda_i M_i \tag{21a}$$

$$U_i^* = \frac{1}{2}\lambda_i^* M_i^* \tag{21b}$$

where M_i and M_i^* are the i^{th} modal masses; λ_i and λ_i^* are the i^{th} eigenvalues. It is assumed that the i^{th} modal mass remains unchanged during the damaging event. Then, the relationship between the quantities U_i and U_i^* is simplified as

$$\frac{U_i}{U_i^*} = \frac{\lambda_i}{\lambda_i^*} \tag{22}$$

By substituting Eq. (22) into Eq. (20), a damage localization index η_j of the j^{th} caisson is computed for *nm* measured modes as follows

$$\eta_j = \frac{\sum_{i=1}^{nm} \phi_{ij}^{2*} \lambda_i}{\sum_{i=1}^{nm} \phi_{ij}^2 \lambda_i^*} \tag{23}$$

in which the components of the right hand side of Eq. (23) are measurable from the real caisson structure.

If we treat damage location indices as normally distributed random variables, the normalized damage indices are defined according to the standard rule as

$$Z_j = \frac{(\eta_j - \mu_\eta)}{\sigma_\eta} \tag{24}$$

where μ_η and σ_η are the mean and the standard deviation of the collection of η_j values, respectively. Next, the damage is localized utilizing hypothesis testing. The null hypothesis (i.e., H_o) is that the

structure is undamaged at the j^{th} element and alternate hypothesis (i.e., H_1) is that the structure is damaged at the j^{th} element. For damage localization, the following decision rule is defined: first, select H_1 if $Z_j < Z_o$; or choose H_o if $Z_j > Z_o$, where Z_o is statistical confidence level of the localization test.

4.2 Verification of MSE-based damage detection

4.2.1Description of simulated damage

As a damage scenario, it is assumed that the structure-foundation interface of the caissons is scoured under extreme wave loading. Three damage cases of the foundation (i.e., Damage 1, Damage 2 and Damage 3) are simulated by removing armor gravel elements as shown in Fig. 17. Only single damage is made in each damage scenario. The percentage loss of the gravel layer of Caisson 1 in Damage 1, of Caisson 2 in Damage 2 and of Caisson 3 in Damage 3 are 2.7%, 10.5% and 6.9%, respectively. In Damage 2 and Damage 3, the damaged areas are expanded to the foundation-caisson contact region.

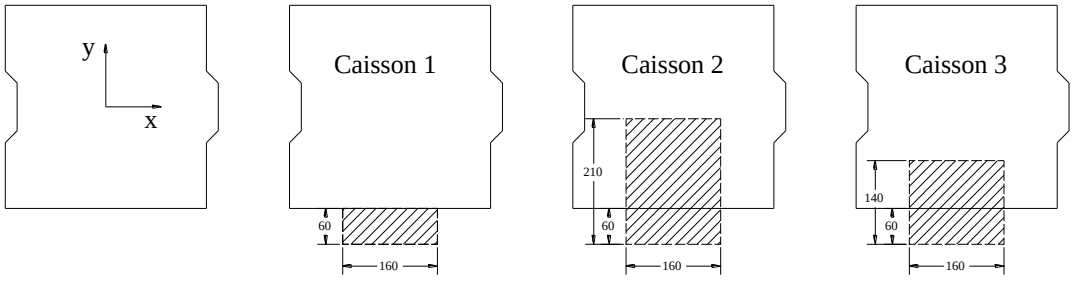

(a) Undamaged (b) Damage 1 (c) Damage 2 (d) Damage 3

Fig. 17 Foundation damage cases

4.2.2 Damage detection results

For detecting foundation damage, y-directional acceleration signals of the points 2, 5 and 8 of the 3-D FE model (see Fig. 5) before and after the damaging event are measured. Next, the natural frequencies and mode shapes are extracted from those signals (by FDD method). Table 4 summarizes the natural frequencies of the caisson system for all damage cases. Only the first and the second modes are listed due to that these modes well match with those of the simplified model. As given in the table, natural frequencies are decreased according to the damage growth. Fig. 18 shows the y-directional mode shapes of the 3-D FE model. It is observed that the relative motions between caissons are changed after the damaging events, and the first mode is more sensitive to the foundation damage than the second one.

Next, the MSE-based method is employed to predict damage locations in the 3-D FE model. The normalized damage index is calculated by Eqs. (23) and (24). Damage localization results are illustrated in Fig. 19. Here, the criterion value Z_o is chosen as 1.26 which is corresponding to the confidence level of 90%. It is found that for all damage cases with different damage severities, the MSE-based method has successfully localized the damaged caissons.

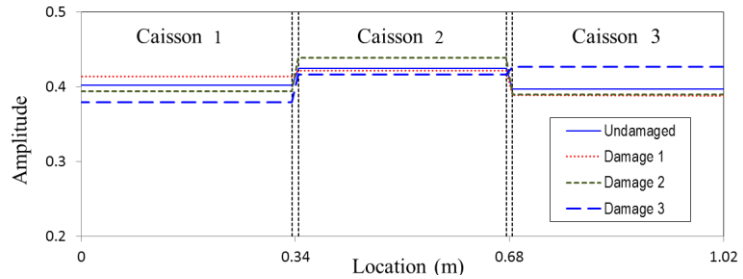

(a) Model 1

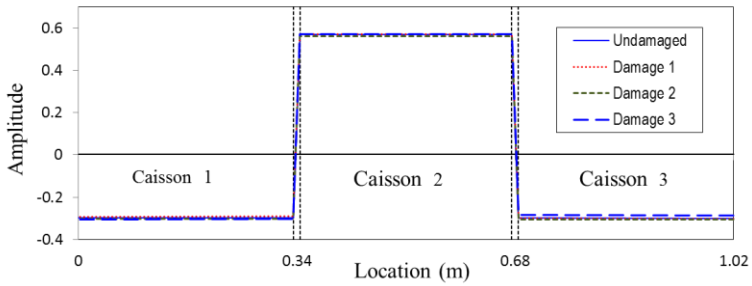

(b) Mode 2

Fig. 18 Y-directional mode shapes of 3-D FE model with foundation damage

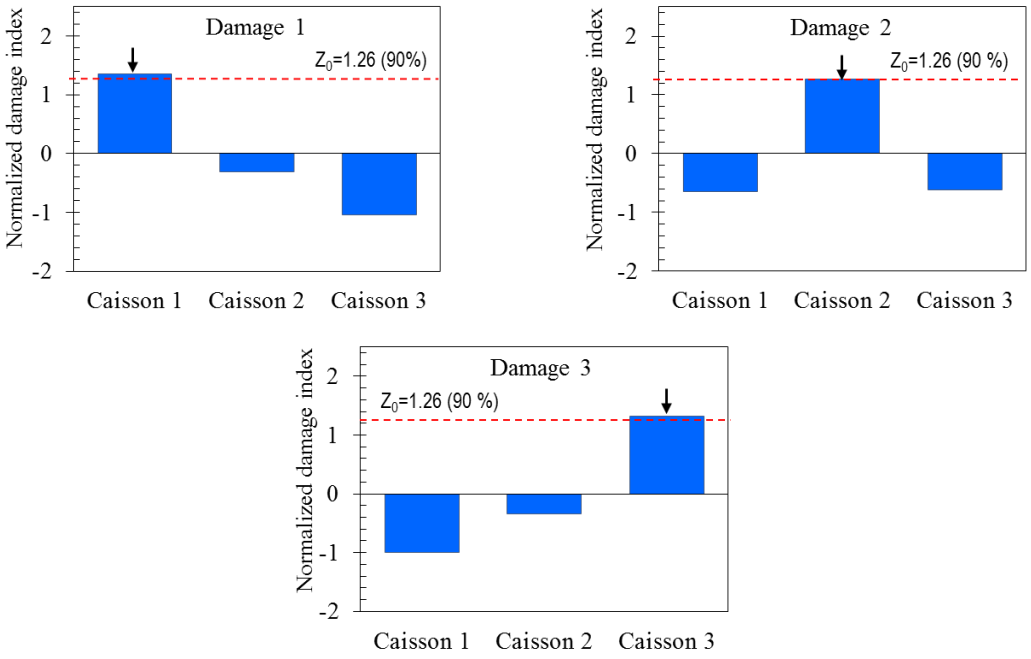

Fig. 19 Damage localization results in 3-D FE model

Table 4 Natural frequencies of 3-D FE model with foundation damage

Case	Damage scenario	Natural frequency (Hz)	
		Mode 1	Mode 2
Undamaged	-	25.33	47.59
Damage 1	Removed 2.7% of armor gravel	25.13 (-0.78%)	47.54 (-0.11%)
Damage 2	Removed 10.5% of armor gravel	24.77 (-2.25%)	46.98 (-1.31%)
Damage 3	Removed 6.9% of armor gravel	24.85 (-1.92%)	47.43 (-0.33%)

*Parentheses indicate variation of natural frequencies with respect to undamaged case

5. Conclusions

In this study, a simplified planar model was developed for damage estimation of interlocked caisson system. The following approaches were performed. Firstly, a conceptual dynamic model of the interlocked caisson system was designed on the basis of the characteristics of existing harbor caisson structures. A mass-spring-dashpot model allowing only the sway motion was formulated. To represent the condition of interlocking mechanism, each caisson unit was connected to adjacent ones via springs and dashpots. Secondly, the accuracy of the planar model's vibration responses was numerically evaluated for a 3-D FE model of interlocked caissons. Finally, the simplified planar model was employed for damage estimation in the interlocked caisson system. For localizing damaged caissons, a damage detection method based on modal strain energy was formulated for the caisson system.

The following observations have been made from numerical tests on the 3-D FE model of the caisson system. Firstly, the proposed planar model successfully estimated the horizontal vibration of the caisson system. The vibration features (i.e., power spectral density, natural frequency and mode shape) of the simplified model were well consistent with those of the 3-D FE model. Hence, the planar model was reliable for the dynamic analysis of the caisson system. Secondly, the MSE-based damage detection method formulated for the simplified planar model successfully identified damage locations with high confidence level.

Despite the feasibility of the proposed planar model of the caisson system for vibration analysis and damage estimation, several issues still remain: (1) the damage severity in the foundation should be studied extensively by quantifying its magnitude; (2) the simplified planar model should be experimentally verified on real or lab-scaled caisson breakwaters for structural health assessment; and (3) a more complex simplified model should be developed to better represent the dynamic behavior of the caisson system subjected to realistic wave action.

Acknowledgements

This work was supported by Basic Science Research Program through the National Research Foundation of Korea (NRF) funded by the Ministry of Education, Science and Technology (NFR-2013R1A1A2A10012040). The authors also would like to acknowledge the financial support of the project 'Development of inspection equipment technology for harbor facilities' funded by Korea Ministry of Land, Transportation, and Maritime Affairs.

References

Bowles, J.E. (1996), *Foundation analysis and design* ,5th Ed., McGraw-Hill.

Chou, J.H., and Ghaboussi, J. (2001), "Genetic algorithm in structural damage detection", *Comput. Structures*, **79**, 1335-1353.

Doebling. S.W., Farrar, C.R. and Prime, M.B. (1998), "A summary review of vibration-based damage identification method", *Shock Vib*., **30**(2), 91-105.

Franco, L. (1994), "Vertical breakwaters: the Italian experience", *Coast. Eng.*, **22**, 3-29.

Gao, M., Dai, G.Y. and Yang, J.H. (1988), "Dynamic studies on caisson-type breakwaters", *Proceedings of the 21st Conference on Coastal Engineering*, Torremolinos, Spain.

Glisic, B., Inaudi, D., Lau, J.M., Mok, Y.C. and Ng, C.T. (2005), "Long-term monitoring of high-rise buildings using long-gage fiber optic sensors", *Proceedings of the 7th International Conference on Multi-Purpose High-Rise Towers and Tall Buildings*, Dubai, UAM.

Goda, Y. (1994), "Dynamic response of upright breakwater to impulsive force of breaking waves", *Coast. Eng.*, **22**, 135-158.

Ho, D.D., Lee, P.Y., Nguyen, K.D., Hong, D.S., Lee, S.Y., Kim, J.T., Shin, S.W., Yun, C.B. and Shinozuka, M. (2012), "Solar-powered Multi-scale Sensor Node on Imote2 Platform for Hybrid SHM in Cable-stayed Bridge", *Smart Struct. Syst.*, **9**(2), 145-164.

Jang, S.A., Jo, H., Cho, S., Mechitov, K.A., Rice, J.A., Sim, S.H., Jung, H.J., Yun, C.B., Spencer, Jr., B.F., and Agha, G. (2010), "Structural health monitoring of a cable-stayed bridge using smart sensor technology: deployment and evaluation", *Smart Struct. Syst.*, **6**(5-6), 439-459.

Kim, D.K., Ryu, H.R., Seo, H.R. and Chang, S.K. (2005), "Earthquake response characteristics of port structure according to exciting frequency components of earthquakes (in Korean)", *J. Korean Soc. Coast.Ocean Eng.*, **17**(1), 41-46.

Kim, J.T. and Stubbs, N. (1995), "Damage localization accuracy as a function of model uncertainty in the I-40 bridge over the Rio Grande", *Proceedings of the SPIE*, San Diego, USA.

Kim, J.T., and Stubbs, N. (2002), "Improved damage identification method based on modal information", *J. Sound Vib.*, **252**(2), 223-238.

Kobayashi, M., Tersashi, M. and Takahashi, K. (1987), "Bearing capacity of rubble mound supporting a gravity structure", *Report Port Harbor Res. Inst.*, **26**(5), 234-241.

Koo, K.Y., Lee, J.J., Yun, C.B. and Kim, J.T. (2009), "Damage detection in beam-like structures using deflections obtained by modal flexibility matrices", *Adv. Sci. Technol.*, **56**, 483-488.

Lamberti, A. and Martinelli, L. (1998) "Prototype measurements of the dynamic response of caisson breakwaters" , *Proceedings of the 26th ICCE,* Copenhagen, Denmark.

Lee, S.Y., Lee, S.R. and Kim, J.T. (2011), "Vibration-based structural health monitoring of harbor caisson Structure" , *Proceedings of the SPIE*, USA.

Lee, S.Y., Nguyen, K.D., Huynh, T.C., Kim, J.T., Yi, J. H. and Han, S.H. (2012), "Vibration-based damage monitoring of harbor caisson structure with damaged foundation-structure interface", *Smart Struct. Syst.*, **10**(6), 517-547.

Look, B. (2007), *Handbook of geotechnical investigation and design tables*, *Taylor & Francis.*

Maddrell, R. (2005), "Lessons re-learnt from the failure of marine structures", *Proceedings of the International Conference on Coastlines, Structures and Breakwaters*, ICE, 139-152.

Marinski, J.G. and Oumeraci, H. (1992), "Dynamic response of vertical structures to breaking wave Forces – review of the CIS design experience", *Proceedings of the 23rd Int. Conf. Coastal Eng., Venice*, ASCE, New York.

Martinelli, L. and Lamberti, A. (2011), "Dynamic response of caisson breakwaters: suggestions for the equivalent static analysis of a single caisson in the array", *Coast. Eng.*, **53**, 1-20.

Matlab R2012b, Inc. (2012), *http://www.matlab.com*

Otte, D., Van de Ponseele, P. and Leuridan, J. (1990), "Operational shapes estimation as a function of dynamic loads", *Proceedings of the 8th IMAC*, Florida, USA.

Oumeraci, H. (1994), "Review and analysis of vertical breakwater failures – lessons learned", *Coast. Eng.*, **22**, 3-29.
Oumeraci, H. and Kortenhaus, A. (1994), "Analysis of the dynamic response of caisson breakwaters", *Coast. Eng*., **22**, 159-183.
Oumeraci, H., Kortenhaus, H., Allsop, W., de Groot, M., Crouch, R., Vrijling, H. and Voortman, H. (2001), *Probabilistic design tools for vertical breakwaters*, Swets & Zeitlinger B.V., Lisse.
Pandey, A.K. and Biswas, M. (1994), "Damage detection in structures using changes in flexibility", *J. Sound Vib.*, **169**(1), 3-17.
Park, J.H., Kim, J.T., Hong, D.S., Ho, D.D. and Yi, J.H. (2009), "Sequential damage detection approaches for beams using time-modal features and artificial neural networks", *J. Sound Vib.*, **323**(1), 451-474.
Park W.S., Lee, S.R., Lee, S.Y. and Kim, J.T. (2011), "Damage monitoring in foundation-structure interface of harbor caisson using vibration-based autoregressive model", *J. Korean Soc. Coast. Ocean Eng.*, **23**(1), 18-25.
Press, W.H., Flannery, B. P., Teukolsky, S.A. and Vetterling, W.T. (1988), *Numerical recipes – the art of scientific computing*, Cambridge University Press, Cambridge.
Richart, F.E., Hall Jr., J.R. and Woods, R.D. (1970), *Vibration of soils and foundations*, Prentice Hall Inc..
SAP2000, Inc. (2006), *http://www.sap2000.org*
Sekiguchi, H. and Ohmaki, S. (1992), "Overturning of caisson by storm waves", *Soild Found*., **32**(3), 144-155.
Sekiguchi, H. and Kobayashi, S. (1994), "Sliding of caisson on rubble mound by wave force", *Proceedings of the 13rd Int. Conf. on Soil Mech. And Found. Eng.*., Balkema, Rotterdam, The Netherlands.
Smirnov, G.N. and Moroz, L.R. (1983), "Oscillations of gravity protective structures of a vertical wall type", *IAHR, Proceedings of the 20th Congress*, **7**, 216-219.
Sohn, H., Farrar, C.R., Hemez, F.M., Shunk, D.D., Stinemates, D.W. and Nadler, B.R. (2003), *A review of structural health monitoring literature: 1996-2001*, Los Alamos National Laboratory Report LA-13976-MS.
Tanimoto, K. and Takahashi, S. (1994), "Design and construction of caisson breakwaters – the Japanese experience", *Coas. Eng*., **22**, 3-29.
Taro, A., Masaharu, S., Ken-ichiro, S., Takashi, T., Daisuke, T., Geyong-Seon, Y. and Kenya, T. (2012), *Investigation of the failure mechanism of kamaishi breakwaters due to tsunami – initial report focusing on hydraulic characteristics*, *Technical Note of The Port and Airport Research Institute*, No. 1251.
Vink, H.A.Th. (1997), *Wave impacts on vertical breakwaters*, *Master's thesis*, Faculty of Civil Engineering, Delft University of Technology, The Netherlands.
Westergaard, H.M. (1933), "Water pressures on dams during earthquakes", *T. Am. Soc.*, **98**(2), 418-432.
Wilson, E.L. (2004), *Static and dynamic analysis of structures*, 4th Ed., *Berkeley, CA: Computers and Structures, Inc.*
Wong, K.Y. (2004), "Instrumentation and health monitoring of cable-supported bridges", *Struct. Health Monit.*, **11**(2), 91-124.
Wu, X, Ghaboussi, J. and Garret, J.H., Jr. (1992), "Use of neural networks in detection of structural damage", *Comput. Struct*., **42**(4), 649-659.
Yamamoto, M., Endo, T., Hasegawa, A. and Tsunakawa, K. (1981), "Random wave tests on a damaged breakwater in Himekawa Harbor, Japan", *Coast. Eng*., **5**, 275-294.
Yang, Z., Elgamal, A., Abdoun, T. and Lee, C.J. (2001), "A numerical study of lateral spreading behind a caissontype quay wall", *Proceedings of the 4th Int. Conf. on Recent Adv. in Geot. Earthq. Eng. and Soil Dyn. and Symp*., California, USA.
Yi, J.H. and Yun, C. B (2004), "Comparative study on modal identification methods using output-only information", *Struct. Eng. Mech*., **17**(3-4), 445-456.
Yoon, H.S., Lee, S.Y., Kim, J.T. and Yi, J.H. (2012), "Field implementation of wireless vibration sensing system for monitoring of harbor caisson breakwaters", *Int. J. Distrib. Sensor Net.*, **2012**, 1-9.
Yun, C.B. and Bahng, E.Y. (2000), "Substructural identification using neural networks", *Comput. Struct*,, **77**(1), 41-52.